encit 2020

ABCM
Associação Brasileira de Engenharia e Ciências Mecânicas

18th Brazilian Congress of Thermal Sciences and Engineering
November 16-20, 2020 (Online)

ENC-2020-0712
CORRELATION OF TWO-PHASE PRESSURE DROP OF THE R1234YF IN SMOOTH HORIZONTAL TUBES: AN ARTIFICIAL INTELLIGENCE APPROACH

Ali Khosravi
Department of Mechanical Engineering, Aalto University, Finland
ali.khosravi@aalto.fi

Juan Jose Garcia Pabon
Institute of Mechanical Engineering, Federal University of Itajuba, Brazil
jjgp@unifei.edu.br

Marcos Felipe Machado Silva
School of Mechanical Engineering, University of Itaúna, Brazil
marcosfelipems21@gmail.com

Mamdouh El HAJ Assad
Department of Sustainable and Renewable Energy Engineering, University of Sharjah, UAE
massad@sharjah.ac.ae

Mohammad Malekan
Department of Engineering, Aarhus University, 8000 Aarhus C, Denmark
mmalekan1986@gmail.com

Abstract. *High global warming potential (GWP) refrigerants that have been used as working fluids in industrial and residential applications are alleged to pose a threat to the environmental security. R134a refrigerant is the most widely used refrigerant medium temperature with GWP of 1430, which therefore must be replaced. One substitute is the R1234yf refrigerant with a GWP lower than 1. In this study, pressure drop during evaporation of R1234yf refrigerant in smooth horizontal tubes is investigated by experimental study and developing intelligent methods. Calculation of the pressure drop for two-phase flow in evaporation and condensation processes needs many experimental tests. Therefore, in this investigation, machine learning algorithms (MLAs) are employed to predict the pressure drop during evaporation of R1234yf refrigerant. Three methods of MLAs are developed to predict the target. These methods are adaptive neuro-fuzzy inference system (ANFIS), ANFIS optimized with particle swarm optimization (ANFIS-PSO), and ANFIS optimized with genetic algorithm (ANFIS-GA). The intelligent models are constructed based on tube diameter (3.2, 4.8, 6.4, and 8 mm); saturation pressure, mass velocity and quality of vapor as input variables and the pressure drop is selected to be the target. The results demonstrated that increasing the mass velocity increases the pressure gradient. Also, for the larger value of tube diameter, the pressure drop has lower values. The behavior of two-phase pressure drop was accurately predicted by the ANFIS-PSO model. Moreover, the PSO algorithm for increasing the performance prediction of the ANFIS model performs better than the GA.*

Keywords: *Pressure drop; R1234yf refrigerant; Adaptive neuro-fuzzy inference system; Particle swarm optimization; Genetic algorithm.*

1. INTRODUCTION

A new generation of refrigerants seems to be driven by scientific findings, regulatory requirements and market pressure (J. Garcia et al, 2018). Greenhouse gases maintained in the atmosphere of the Earth results in global warming. This amount of heat that causes this warming is called global warming potential (GWP). The GWP is defined as one major selection criteria for the new generation of refrigerants (A. Khosravi et al, 2018). There are different refrigerating fluids that are presently known to mankind which are used in a specific thermodynamic cycle. Obtaining the high energy efficiency in addition to the low GWP is an important issue to alternate a new refrigerant instead of previous refrigerants. R1234yf is foreseen to be a replacement for R134a in automobile air conditioning systems after the European Commission directed a phase-out for R134a. The properties of the R1234yf are low GWP, low toxicity, low flammable, its vapor pressure is similar to that for R134a, and the ratio of operating pressure for R1234yf is 40% lower than that for R410A.

A wide application in the modern industry can be mentioned for two-phase flow. From the vast industrial application, two-phase flow is applied in refrigeration systems, air conditioning, petroleum, and food industry. Most of the applications require the ability to forecast the two-phase frictional pressure drop accurately for the design and optimization of components such as pumps, heat exchangers and pipelines.

Two-phase flow pressure drop depends on several design parameters (such as diameter, vapor quality, mass velocity, etc.). In this study, the two-phase pressure drop during evaporation of R1234yf is evaluated using experimental study and intelligent methods. Indeed, intelligent models are employed to catch hidden and strongly non-linear dependencies of two-phase flow of the low GWP R1234yf refrigerant under different design parameters. Based on the literature, for prediction of heat transfer coefficient and pressure drop in two-phase flow of refrigerants, MLP neural network was employed as the intelligent model. For this method, some imperfections have been reported that are slow convergence, overfitting, and poor generalizing performance. This study for the first time proposes the ANFIS-PSO and ANFIS-GA methods to predict the pressure drop of two-phase flow of refrigerants. Indeed, the main contribution of this study is to develop an accurate, fast, and reliable model of MLAs to predict the two-phase flow pressure drop of R1234yf. Also, this study provides a comparison between PSO and GA algorithms to improve the prediction accuracy of the ANFIS method, which can be used to study the behavior of two-phase flow fluids.

2. EXPERIMENTAL SETUP

The schematic diagram of the experimental setup is shown in Fig. 1. A configuration was applied to measure the pressure drop of R1234yf. A copper tube with an internal diameter of 4.8 mm was used for the refrigeration loop as well as a self-lubricating oil-free gear micro-pump was used to deliver subcooled refrigerant to the heater. First, the working fluid (here R1234yf refrigerant) is preheated and partially evaporated in the heater and then passes through the test section and is condensed and subcooled in the condenser. To obtain the fluid conditions, the thermocouples and pressure transducers were in different positions.

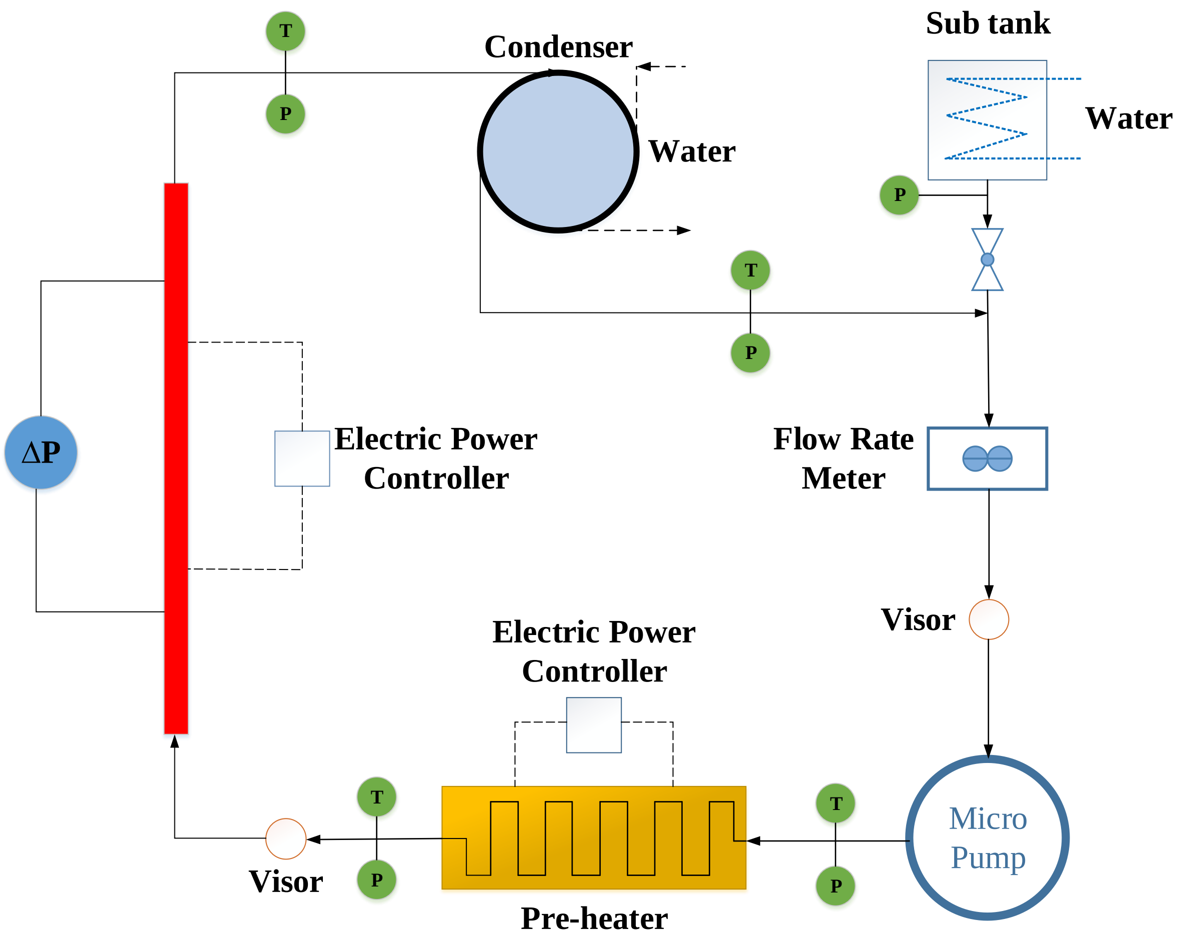

Figure 1. Schematic diagram of experimental setup.

A fully developed flow condition is measured by a tube that is located upstream of the tube. To calculate pressure drop across the tube a differential pressure transducer with an accuracy of 2.8 kPa was used. The test section has an electrical resistance wrapped on the exterior surface, which provides a maximum heat flux of 15 kW/m². All tests were carried out under steady-state conditions of mass velocity, entire range of vapor quality and saturation pressure. The data are recorded by a computer and LabVIEW Software. The Table 1 are the summaries of the experimental conditions in the present study.

Table 1. Experimental conditions evaluated in the present study.

Fluid	$\boldsymbol{D}\ (\boldsymbol{mm})$	$\boldsymbol{T_{sat}}(°\boldsymbol{C})$	$\boldsymbol{G}(\boldsymbol{kg/m^2s})$
R1234yf	3.2	20	200, 300, 400
	4.8	20, 30	200, 300, 400
	6.4	20, 30	200, 300
	8.0	20, 30	200, 300

3. PRESSURE DROP CALCULATION

The pressure gradient is determined as the ratio between the pressure drops in smooth and horizontal tubes were measured and divided by the length:

$$\frac{dP}{dz} = \frac{\Delta P}{L} \tag{1}$$

The mass velocity is:

$$G = \frac{4\dot{m}}{\pi D^2} \tag{2}$$

in which $\dot{m}$ is the mass flow rate and D is the internal diameter of the tube. By applying the energy balance over the preheater, the vapor quality at the outlet of preheater is calculated based on the following equation.

$$x_{ph,out} = \frac{1}{i_{lv,ph,out}}\left(\frac{\dot{Q}_{ph}}{\dot{m}} - \left(i_{l,ph,out} - i_{ph,in}\right)\right) \tag{3}$$

In where $i_{ph,in}$ is the liquid enthalpy at the preheater inlet, i_l and i_{lv} are the saturated liquid enthalpy and heat of vaporization corresponding to the saturation temperature at the preheater exit (test section inlet).

The preheater heat transfer rate, $\dot{Q}_{ph}$, is

$$\dot{Q}_{ph} = \eta_{ph} V_{ph} I_{ph} \tag{4}$$

in which V_{ph} is the voltage, I_{ph} is the current electrical applied in the preheater, η_{ph} is the efficiency between heat and electrical power in the preheater (for single-phase experimental tests is considered to be 0.93).

4. MACHINE LEARNING ALGORITHM

The intelligent methods are developed based on the experimental data (inputs: $4 \times 212 = 848$, target=212). The experimental data are divided into two sections that are train dataset (70%) and test dataset (30%). Three statistical indicators are used to calculate the performance prediction of the intelligent methods. These statistical indices are root mean square error (RMSE), correlation coefficient (R) and mean square error (MSE), which are expressed as, respectively. In this algorithm RMSE measures the mean square error of the data, on the other hand, MSE presents the dispersion of the calculated value.

$$RMSE = \sqrt{\frac{1}{n}\sum_{i=1}^{n}(x_i - y_i)^2} \tag{5}$$

$$R = \frac{\sum_{i=1}^{n}(x_i - \bar{x})(y_i - \bar{y})}{\sqrt{\sum_{i=1}^{n}(x_i - \bar{x})^2 \sum_{i=1}^{n}(y_i - \bar{y})^2}} \tag{6}$$

$$MSE = \frac{1}{n}\sum_{i=1}^{n}(x_i - y_i)^2 \tag{7}$$

where x_i, y_i, $\bar{x}$, $\bar{y}$ and n are experimental data, predicted data by the intelligent methods, experimental data mean, mean of predicted data mean, and number of data, respectively.

4.1 ANFIS model

ANFIS method is defined as a combination of two soft-computing methods including an artificial neural network (ANN) and fuzzy logic. Indeed, ANN is used to obtain the knowledge of human expert in a fuzzy logic system to determine the design parameters automatically. This combination causes a supervised learning on learning algorithm. For developing an ANFIS method, Takagi-Sugeno fuzzy method is used. This method works better for optimization and adaptive techniques. Figure 2 shows a simple structure of the ANFIS model. This is an example of ANFIS operation with two inputs and one output. For more information about rules and layer in Haznedar and A. Kalinli (2016).

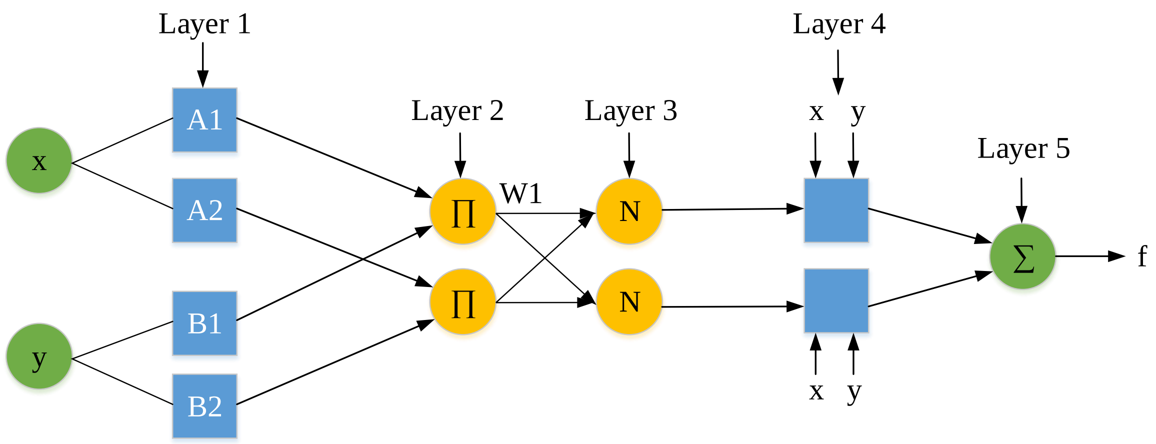

Figure 2. ANFIS model structure diagram.

4.2 PSO algorithm

This method uses a global gradient-less accidental search method in its structure and is suitable for continues variable problems. The PSO algorithm maintains multiple potential solutions at one time (A. Khosravi et al, 2018). Objective function is used to determine the fitness of each solution during each iteration. Each solution is expressed by a particle in the fitness search space. Objective function returns the particles “swarm” or “fly” through the search space to find the maximum. Figure 3 shows a structure of PSO algorithm.

Each PSO algorithm follows three main targets which are: The first one is the target that is the main subject to develop a PSO algorithm, the second one is global best (gBest) value that detectives which particle’s data is currently closer to the target and the third one is the stop condition of the algorithm.

Moreover, each particle contains three vectors and one parameter, these are:

1. $\vec{x}_i$: is particle *i* current position in the search space
2. $\vec{p}_i$: is particle *i* best position in history
3. $\vec{v}_i$: is particle *i* velocity
4. $pBest_i$: is solution quality of particle *i* which has the best position

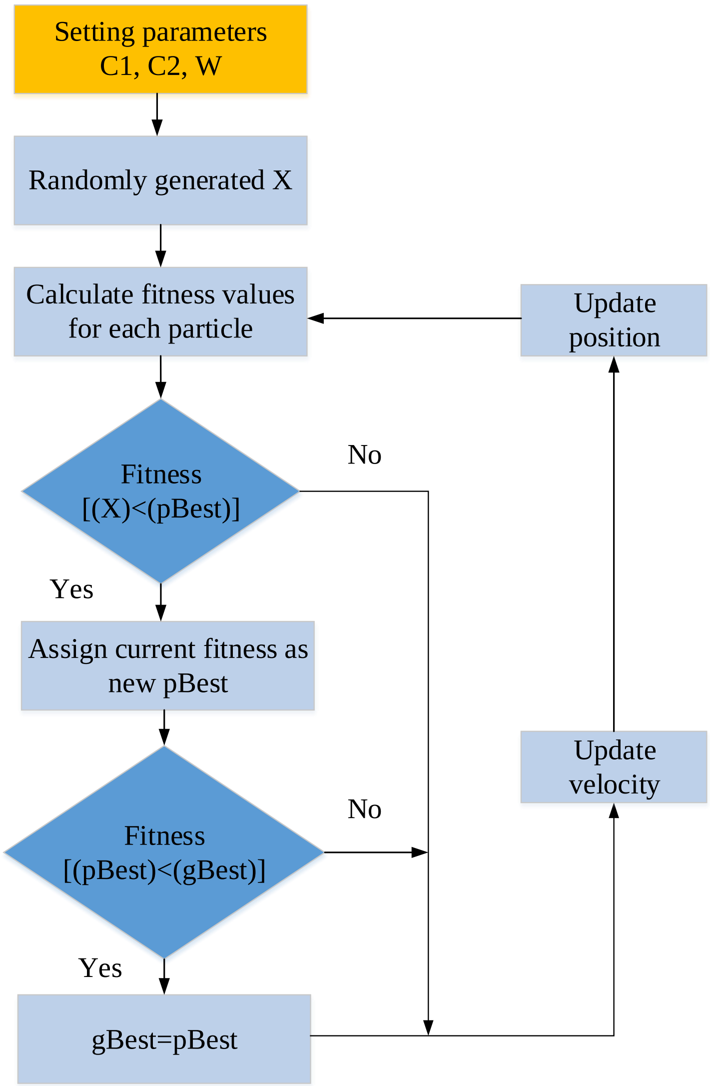

Figure 3. Flow diagram of PSO algorithm.

4.3 Genetic algorithm (GA)

This algorithm is defined as a search technique to find the true solution or approximately optimum solution for each problem. This process is carried out based on the inspiration of evolutionary biology such as inheritance, mutation, selection and crossover. The evaluation commonly is carried out from a population of randomly generated individuals and happens in generations. In the first step, the fitness of every individual in the population is assessed (in each generation), multiple individuals are selected from the current population and modified to form a new population. After that, in the next iteration, a new population is used. The algorithm will be finished when either a maximum number of generations has been generated, or a satisfactory fitness level has been reached for the population.

5. RESULTS AND DISCUSSION

The correlation of Xu and Fang (2012) was used to validate the experimental data. The results show that the determination correlation between the experimental and predicted data is approximately $R^2 = 0.95$. This value of determination coefficient shows that there is a good agreement between the predicted and experimental data.

For prediction of two-phase pressure drop during evaporation of R1234yf, some intelligent methods were implemented by Matlab Software. The first method is ANFIS. For this model, finding the optimum number of clusters can help to reach the best performance of the model. Although the predicted data by the ANFIS model follow the experimental data, for some points, the magnitude of disagreement is high. Therefore, genetic algorithm was employed to improve the performance prediction of the ANFIS model. Indeed, this optimization algorithm was used to find the optimum value of the ANFIS parameters. Figure 4 demonstrates the train and test data of the ANFIS-GA model for prediction of pressure drop in two-phase flow of R1234yf. As it was quoted the experimental data are divided into two sections that are train dataset (150 data, which represents 70% of the number of targets that is 212) and test dataset (70 data, which represents 30%). It can be concluded that the genetic algorithm increased the prediction accuracy of the ANFIS model and the predicted data by ANFIS-GA model follow the experimental data with a high accuracy. For this prediction, the statistical indices were obtained as RMSE=1.3552 (kPa/m), R=0.9748 and MSE=1.8366 (kPa/m), for testing phase of the network.

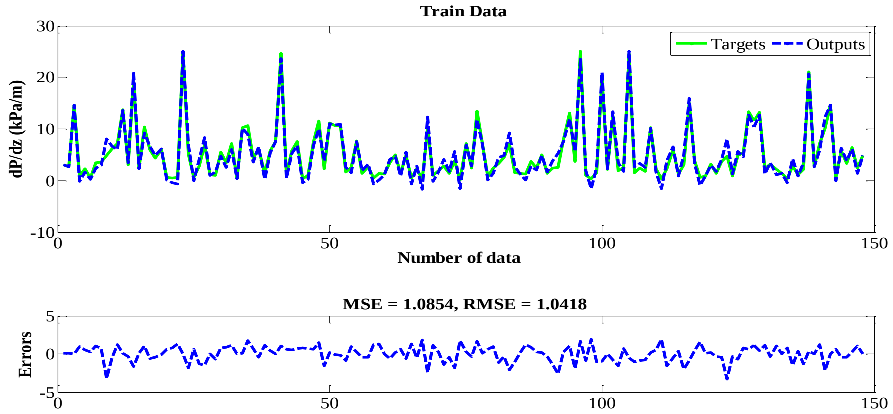

(a) 150 data

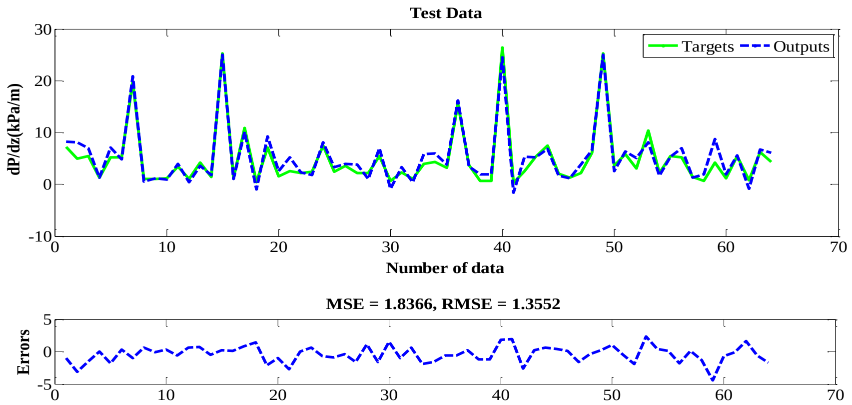

(b) 70 data

Figure 4. Train and test data of the ANFIS-GA model for prediction of pressure drop for two sets of data.

The second algorithm that was considered to optimize the ANFIS model is the PSO algorithm. As explained before, genetic algorithm successfully increased the prediction accuracy of the ANFIS model. Here, a comparison is carried out between the genetic and PSO algorithms for optimization of the ANFIS model. Training and testing phases of the ANFIS-PSO model is shown in Figure 5. As can be seen in the figure, predicted data by the ANFIS-PSO model have a good agreement with the experimental data. This prediction shows the performance compared to the ANFIS and ANFIS-GA models and the statistical indices were calculated as RMSE=0.6992 (kPa/m), R=0.9919 and MSE=0.4888 (kPa/m) (for test datasets).

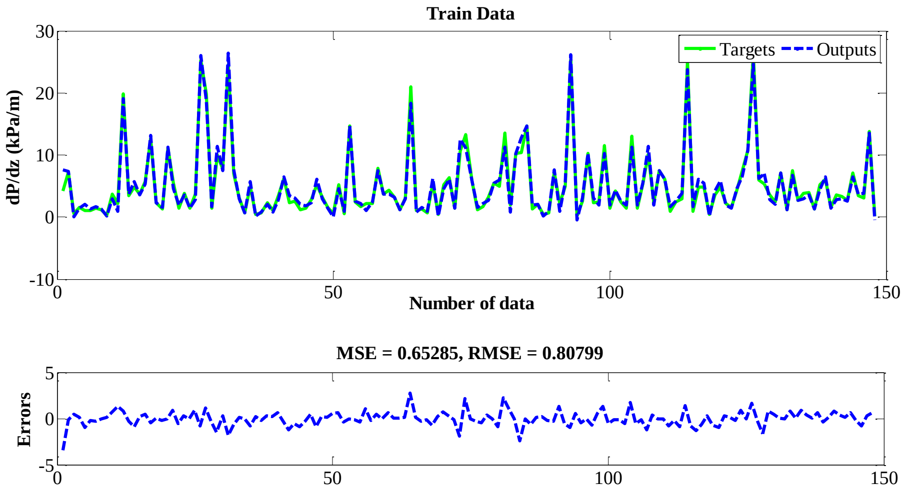

(a) 150 data

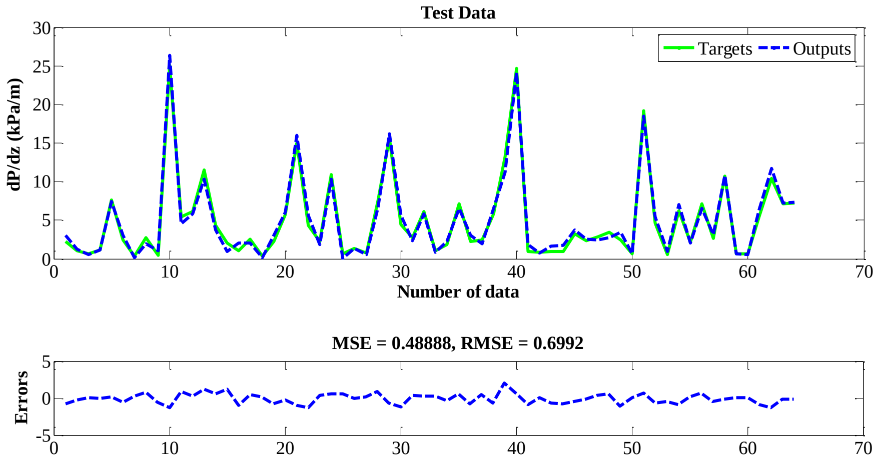

(b) 70 data

Figure 5. Training and testing phases of the ANFIS-PSO method for two sets of data.

Figure 6 shows the variation of mass velocity versus vapor quality of refrigerant for the tubes with 4.8 mm diameters. For this analysis, the saturation pressure is 5.917 bar (in adiabatic condition). Regarding the figure, pressure drop during evaporation of R1234yf increases by increasing the mass velocity. Increasing the mass velocity promotes the slippage between the liquid and vapor velocities that it raises the interfacial friction and resulting in a greater pressure drop in the same quality. In addition, increasing the vapor quality (between 0 and 0.8) rises the pressure drop in which the maximum pressure drop occurs at x=0.8. Of course, this increasing becomes more evident and highlighted by increasing the mass velocity. Also, this figure shows that the ANFIS-PSO model accurately predicts the pressure drop during evaporation of R1234yf and the magnitudes of disagreement between predicted and experimental data are low.

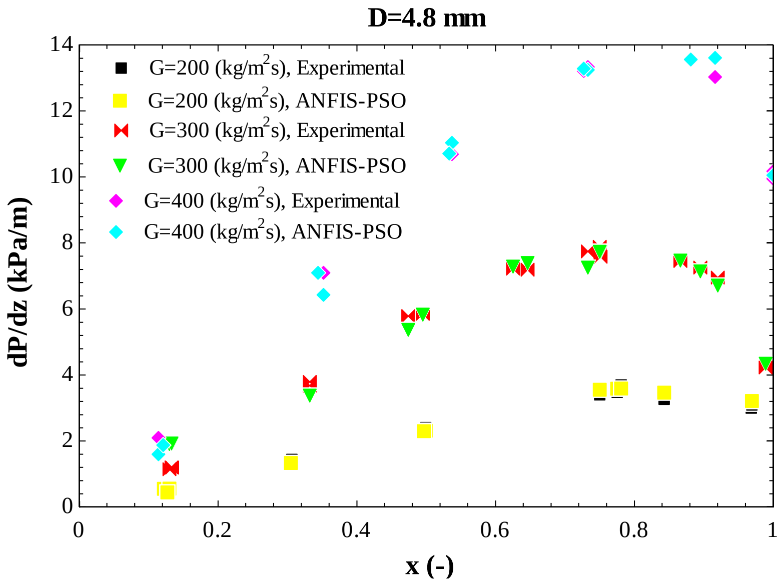

Figure 6. Variation of mass velocity versus vapor quality.

The variation of pressure drop along with vapor quality for different tube diameter is shown in Figure 7. This figure shows that the value of pressure drop by increasing the tube diameter decreases. It is important to mention that when the tube diameter decreases from 6.4 mm to 4.8 mm, the pressure gradient remains approximately the same. But according to the figure, the pressure gradient has a drastic increase by decreasing the tube diameter from 4.8 mm to 3.2 mm. These phenomena are described by the transition from macro-channels into mini-channels. Figure 5 also shows that data obtained by ANFIS-PSO model successfully follow those obtained from the experimental data.

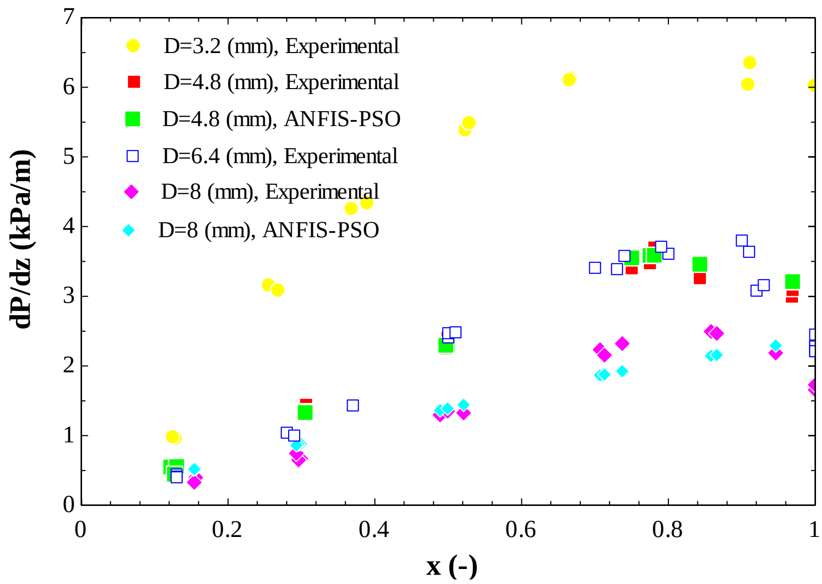

Figure 7. Effect of tube diameter on two-phase pressure gradient of R1234yf versus vapor quality.

Figure 8 demonstrates the ANFIS-PSO decision surface for prediction of two-phase pressure gradient. As before mentioned, for larger tube diameters, the pressure gradient has the lower value as well as increasing the vapor quality (from 0 to the critical point 0.8) increases the two-phase pressure drop. The ANFIS-PSO model represented a continuous surface to predict the behavior of the two-phase pressure gradient of R1234yf. Also, the variation of saturation pressure and mass velocity is in accordance with the experimental data.

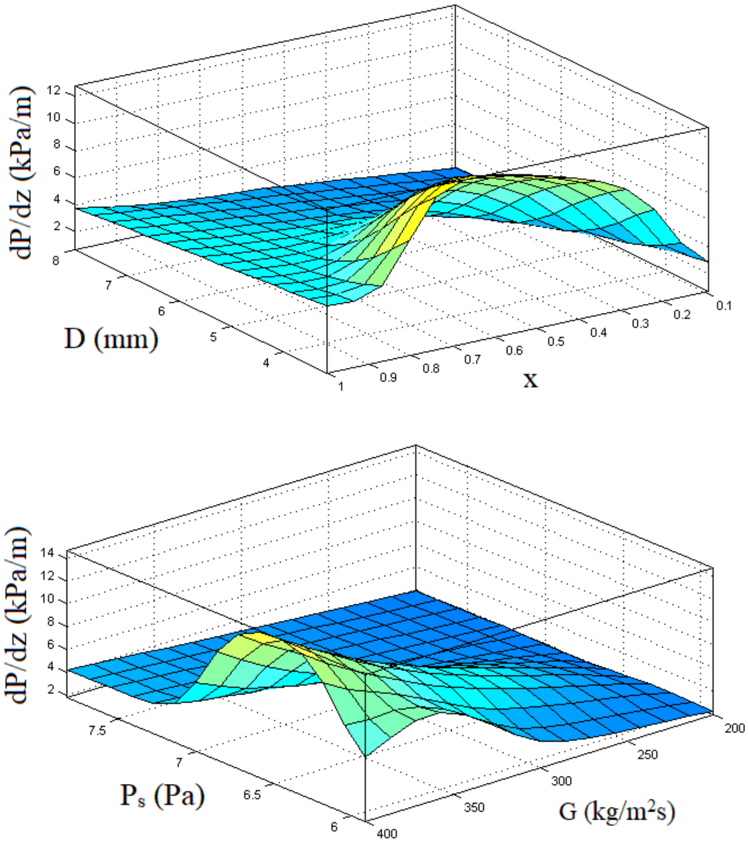

Figure 8. The decision surface of the ANFIS-PSO model for prediction of two-phase pressure drop.

Figure 9 presents a comparison between the statistical indices obtained by ANFIS-PSO model and Xu and Fang (2012). As Figure 9 shows, correlation coefficient between the experimental and predicted data obtained by ANFIS-PSO model is higher than Xu and Fang correlation.

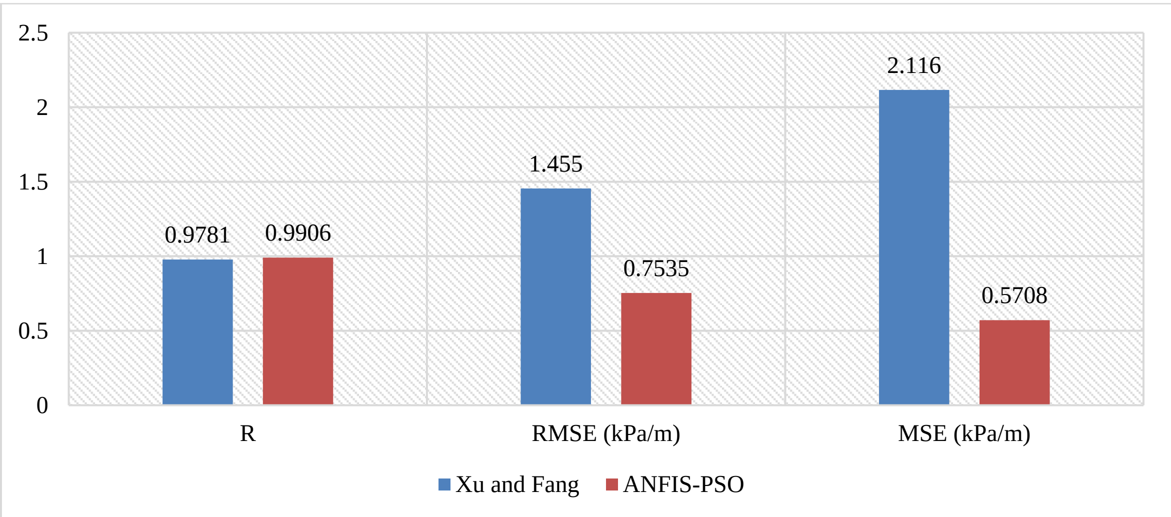

Figure 9. Prediction accuracy by ANFIS-PSO model and Xu and Fang (2012) correlation

6. CONCLUSIONS

In this study, an experimental investigation was carried out to analyze the two-phase pressure drop during evaporation of R1234yf. Based on the experimental data (212 data) three different methods of machine learning algorithms (MLAs) were developed to predict the two-phase pressure gradient. The developed MLAs were adaptive neuro-fuzzy inference system (ANFIS), ANFIS optimized with particle swarm optimization algorithm (ANFIS-PSO) and ANFIS optimized with genetic algorithm (ANFIS-GA). The intelligent methods were constructed based on the tube diameter, mass velocity, vapor quality and saturation pressure as input parameters. The experimental investigation has shown that increasing the mass velocity increases the two-phase pressure gradient. For larger tube diameters the two-phase pressure drop has the lower value. Also, increasing the saturation pressure can increase the two-phase pressure gradient. In addition, intelligent models accurately predicted the two-phase pressure drop during evaporation of R1234yf. The results demonstrated that the optimization algorithms (PSO and GA) successfully increased the performance prediction of the ANFIS model. The best performance was obtained for the ANFIS-PSO model, which the statistical indicators for this model were obtained as RMSE=0.6992 (kPa/m), R=0.9919 and MSE=0.4888 (kPa/m) (for test datasets).

7. ACKNOWLEDGEMENTS

The authors appreciate the support of CAPES, CNPq, and FAPEMIG of Brazil.

8. REFERENCES

J. Garcia, T. Ali, W. M. Duarte, A. Khosravi, and L. Machado, "Comparison of transient response of an evaporator model for water refrigeration system working with R1234yf as a drop-in replacement for R134a," *Int. J. Refrig.*, 2018.

A. Khosravi, R. N. N. Koury, and L. Machado, "Thermo-economic analysis and sizing of the components of an ejector expansion refrigeration system," *Int. J. Refrig.*, vol. 86, pp. 463–479, Feb. 2018.

A. Khosravi, L. Machado, and R. N. Oliviera, "Time-series prediction of wind speed using machine learning algorithms: A case study Osorio wind farm, Brazil," *Appl. Energy*, vol. 224, no. C, pp. 550–566, 2018.

B. Haznedar and A. Kalinli, "Training ANFIS Using Genetic Algorithm for Dynamic Systems Identification," Int. J. Intell. Syst. Appl. Eng., vol. 4, no. Special Issue, pp. 44–47, 2016

R. Revellin, M. Padilla, A. Bensafi, P. Haberschill, and J. Bonjour, "Thermodynamic analysis of a diabatic two-phase flow for a pure refrigerant and a refrigerant/oil mixture under equilibrium conditions," *Int. J. Refrig.*, vol. 32, no. 7, pp. 1784–1790, Nov. 2009.

Y. Xu and X. Fang, "A new correlation of two-phase frictional pressure drop for evaporating flow in pipes," *Int. J. Refrig.*, vol. 35, no. 7, pp. 2039–2050, Nov. 2012

9. RESPONSIBILITY NOTICE